

Manifold-based Proving Methods in Projective Geometry

Michael Martin Katzenberger¹, Jürgen Richter-Gebert²

¹ michael.martin.katzenberger@tum.de, Orcid: 0009-0004-2270-2502

² richter@tum.de, Orcid: 0009-0000-0049-9743

Department of Mathematics, CIT, Technical University of Munich

Abstract. This article compares different proving methods for projective incidence theorems. In particular, a technique using quadrilateral tilings recently introduced by Sergey Fomin and Pavlo Pylyavskyy is shown to be at most as strong as proofs using bi-quadratic final polynomials and thus, also proofs using Ceva-Menelaus-tilings. Furthermore, we demonstrate the equivalence between quadrilateral-tiling-proofs and proofs using exclusively Menelaus configurations. We exemplify the transition between the proofs in several examples in 2D and in 3D.

Keywords: Binomial Proofs · Tilings · Projective incidence theorems · Bracket algebra

1 Introduction

Projective geometry studies properties that are invariant under projective transformations. We here focus on the most basic of such properties: Incidence relations between points and lines (and in 3D also planes). They are natural projective invariants since they are stable under projective transformations. The typical blueprint of a projective incidence theorem reads like:

some incidences hold + some incidences do not hold \implies another incidence holds.

Incidence theorems only including points and lines are an important basic form of planar geometric theorems. By suitable tools many other geometric statements can ultimately be reformulated as theorems of this form and thus be reduced to statements involving points/lines/incidences only.

There is an extensive literature on the automatic generation of proofs in such a context, reaching from very general algebraic tools like Gröbner Bases [6], and Wu’s Method [10] via still general more invariant geometric approaches like *final polynomials* [4] to more specialised methods that exploit specific cancellation patterns in terms of bracket algebra and unveil some of the geometric reasons “why” some theorems do hold. We here are interested in the comparison of the latter class of proving methods.

In this article we will compare (bi-quadratic) final polynomials [4, 9], proofs by manifold structures on Ceva-/Menelaus-configurations [1, 8] and the recently

introduced quadrilateral tiling method by Fomin and Pylyavskyy [7, 5]. All three methods rely on cancellation patterns on the bracket level. The last two methods additionally have in common that the cancellation patterns can be organised on an orientable 2-manifold such that each cancellation corresponds to two patches of the manifold meeting along an edge. The statement that a theorem holds corresponds to the fact that the underlying manifold does not have a boundary. In other words: One has a theorem if everything closes up nicely.

We will quickly recall the established proving methods, present quadrilateral-tiling-proofs and then show that they are at most as powerful as the other techniques.

2 Binomial Proofs and Ceva-Menelaus-Proofs

2.1 Binomial Proofs

As usual we will abbreviate the determinant of three planar points in homogeneous coordinates by $[A, B, C] := \det(p_A, p_B, p_C)$. Binomial proofs have first been introduced in the context of oriented matroid theory [2, 9] and are by now pretty well understood. They utilize bi-quadratic final polynomials coming from Grassmann-Plücker-relations. For any points A, B, C, D, E in the projective plane the following equation holds:

$$[A, B, C][A, D, E] - [A, B, D][A, C, E] + [A, B, E][A, C, D] = 0 \quad (1)$$

This means, that collinearity of A, B and C immediately implies

$$[A, B, D][A, C, E] = [A, B, E][A, C, D]. \quad (2)$$

And on the other hand, if equation (2) holds and we know that A, D, E are not collinear, collinearity of A, B, C is implied. In the binomial proving technique incidences of the hypotheses as well as the conclusion are translated in equations of type (2). A proof consists of a collection of such equations such that the equation that represents the conclusion is obtained from hypotheses equations by multiplying all terms on the left and all all terms on the right and cancelling terms that occur on both sides. The non-incidence statements are used as non-degeneracy conditions to make sure that no division by zero arises along the cancellation process. While this method is not known to work in general it is known for producing short, readable and insightful proofs if it works. Actually to the best of our knowledge it still might be the case that if one allows to add auxiliary points every incidence theorem that holds over arbitrary fields admits a binomial proof. An equivalent question was posed in [5] as Problem 3.3. No proving strategy or counterexample currently seems to be in reach.

2.2 Ceva-Menelaus-Proofs

This proving method introduced in [8] uses multiple instances of Ceva's and Menelaus's theorems to prove incidences. The structure of the proof is organised along a triangulated orientable manifold. Each triangle carries a Ceva or a

Menelaus configuration. Edge points of adjacent triangles are identified. If the corresponding incidence structure of the configuration holds for all but one of the triangles then it will automatically hold for the last triangle, hence a certain incidence theorem holds. Here the length ratios along all edges between two as-

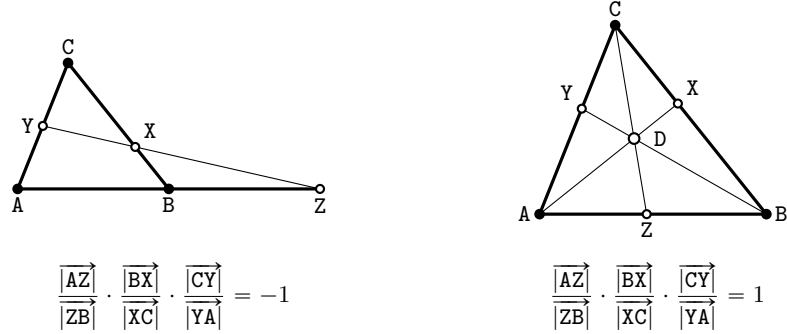


Fig. 1. Menelaus's and Ceva's theorem and their corresponding equations.

signed triangles cancel such that only the length ratios along the boundary of the unassigned triangle remain. This implies that the final triangle must also correspond to either a Ceva or Menelaus configuration forcing an additional incidence (the conclusion) to hold. For more details, see [8]. In [1] a procedure to translate a binomial proof into a Ceva-Menelaus-proof (*CM-proof*, for short) and vice versa is described, showing that these proving techniques are equally powerful, as long as it is allowed to add two auxiliary generic points to the configuration.

3 Quad proofs á la Fomin and Pylyavskyy

In the recent paper “Incidences and Tilings” [7], Fomin and Pylyavskyy introduce another proving technique that also relies on a manifold based approach. Unlike in the Ceva-Menelaus technique in this approach the basic building blocks are quadrilateral tiles, each of them encoding a kind of cross ratio. The idea is to have a variable cancel out whenever two tiles meet along an edge and the conclusion being the last tile to be filled. This is very similar to the Ceva-Menelaus approach. In a certain sense the quadrilateral building blocks are of more elementary nature: The vertices of each quadrilateral face (we will call them quadrangles) represent two points P, Q and two lines l, m not incident to each other and the additional “coherency”-condition that P, Q and $l \wedge m$ are collinear. The collinearity of these three points, or — dually — the concurrency of the 3 lines l, m and $P \vee Q$, is equivalent to the, also self-dual, algebraic expression

$$\frac{\langle P, l \rangle \cdot \langle Q, m \rangle}{\langle P, m \rangle \cdot \langle Q, l \rangle} = 1. \quad (3)$$

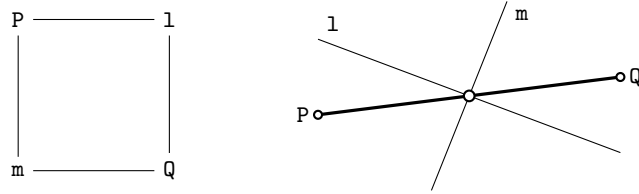


Fig. 2. A coherent quadrangle and the underlying incidence structure.

If one traverses such a quadrangle counter-clockwise, the scalar products corresponding to edges from *line* to *point* appear in the numerator of the fraction and the determinants corresponding to edges from *point* to *line* appear in the denominator of the fraction. This means gluing two counter-clockwise oriented quadrangles along an edge will result in the scalar products coming from this edge appearing once in the numerator and once in the denominator and thus cancel out. So, similar to Ceva-Menelaus-proofs, if in a tiling of a closed oriented surface with these quadrangles, all tiles but one are coherent, the remaining tile will be coherent, too. Thus, every quadrilateral tiling encodes a proof (we will refer to such proofs as *quad-proofs*) of a projective incidence theorem. In [7] many examples of quadrilateral tiling proofs for projective incidence theorems are given. One might guess that this more elementary proving technique provides more general proofs and can prove larger classes of theorems compared to the Ceva-Menelaus techniques. However, it turns out that every quad-proof can be turned to an equivalent proof using Menelaus theorems only.

3.1 Extracting a binomial proof from a quad-proof

As the coherency of a quadrangle is equivalent to an equation being satisfied, it seems natural trying to relate this proving method to binomial proofs. And in fact the process of extracting a binomial proof from a quad-proof is quite straight-forward. By choosing two points L_1, L_2 spanning 1 , two points M_1, M_2 spanning m and defining the incidence point $I = 1 \wedge m$ each coherent quadrangle actually encodes 3 collinearities, yielding the equations

$$\begin{aligned} L_1, L_2, I \text{ col.} &\iff [L_1, L_2, P][L_1, I, Q] = [L_1, L_2, Q][L_1, I, P], \\ M_1, M_2, I \text{ col.} &\iff [M_1, M_2, Q][M_1, I, P] = [M_1, M_2, P][M_1, I, Q] \text{ and} \\ I, P, Q \text{ col.} &\iff [I, P, L_1][I, Q, M_1] = [I, P, M_1][I, Q, L_1]. \end{aligned}$$

The multiplying left and right sides of these equations yields

$$[P, L_1, L_2][Q, M_1, M_2] = [P, M_1, M_2][Q, L_1, L_2], \quad (4)$$

which is equivalent to equation (3). Applying this procedure to each quadrangle thus immediately gives us a binomial proof, so quad-proofs can only be “as powerful as” binomial proofs — and hence also Ceva-Menelaus-proofs. In other words: each quad-proof can be translated into a bi-quadratic proof and from there into a CM-proof.

4 Relations between the Tiling-Based Methods

4.1 Quad-proofs and Ceva-Menelaus-proofs

One way to directly translate quad-proofs into Ceva-Menelaus-proofs is actually already implicitly provided in [7]. There, a translation process to proofs using “triangulations of closed oriented surfaces” is described, that essentially converts a quad-proof into a Ceva-Menelaus-proof using *only* Menelaus-triangles, however without mentioning the theorem of Menelaus explicitly. This is done by first iteratively inserting additional quadrangles in the places of “line-vertices” contained in more than 3 quadrangles by splitting them into 2 vertices, extend-

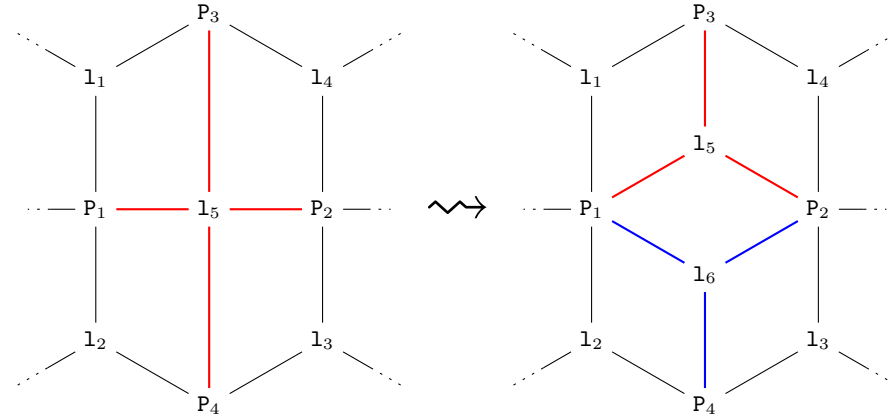


Fig. 3. Splitting a line-vertex by inserting a new quadrangle.

ing the quad-proof to a proof of a more general projective incidence theorem (This more general theorem collapses to the original theorem in case the 2 lines corresponding to the line-vertices coincide). Then, if all line-vertices are contained in exactly 3 quadrangles, the quadrilateral tiling can be translated into a triangulation by splitting all quadrangles in half and gluing triples of halves containing the same line-vertex to triangles, as visualized in Figure 4. It is easy to see that the underlying incidence structure of these triangles is exactly that of the theorem of Menelaus. This procedure can simply be reversed to get from any pure Menelaus-proof to a quad-proof, so quad-proofs and pure Menelaus-proofs are equally powerful.

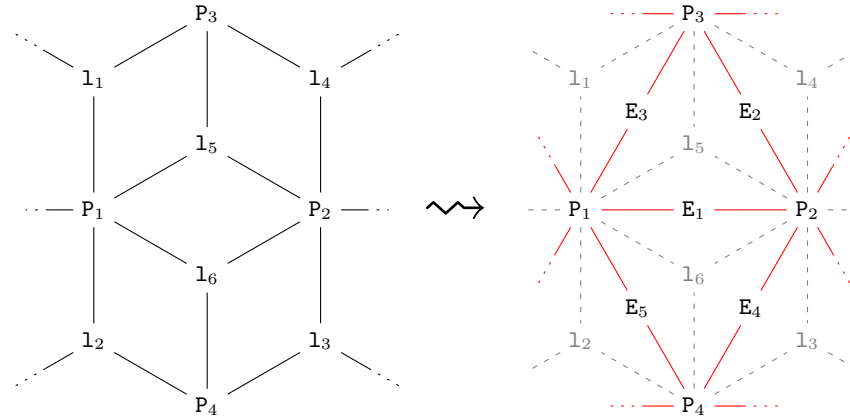


Fig. 4. Translating a quad-proof into a pure Menelaus-proof.

4.2 Ceva vs Menelaus

Naturally the question arises, if pure Menelaus-proofs are already as powerful as Ceva-Menelaus-proofs. It turns out, that Ceva's theorem can actually be combined from two applications of Menelaus's theorem, visualized in Figure 5. However, a simple argument shows that replacing single Ceva-triangles in

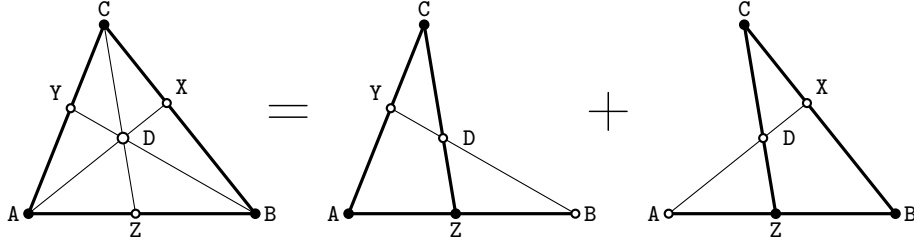


Fig. 5. Proof of Ceva's theorem using Menelaus's theorem twice.

a Ceva-Menelaus-proof by any number Menelaus-triangles is not possible:

1. The total number of triangles is even: Each triangle has 3 edges and each edge is contained in 2 triangles, so $3 \cdot \# \text{triangles} = 2 \cdot \# \text{edges}$.
2. The total number of Menelaus-triangles (thus by 1. also Ceva-triangles) is even: Each Menelaus-triangle adds a factor “-1”, but the product of all equations must be 1.
3. Replacing a single Ceva-triangle by Menelaus-triangles makes the number of Ceva-triangles odd.

Nevertheless, some replacements are possible. If a Ceva-Menelaus-proof contains 2 adjacent Ceva-triangles, both can be split simultaneously into 4 adjacent

Menelaus-triangles sharing the former edge point of the edge between the two Ceva-triangles as a vertex point, as shown below. While this does not allow

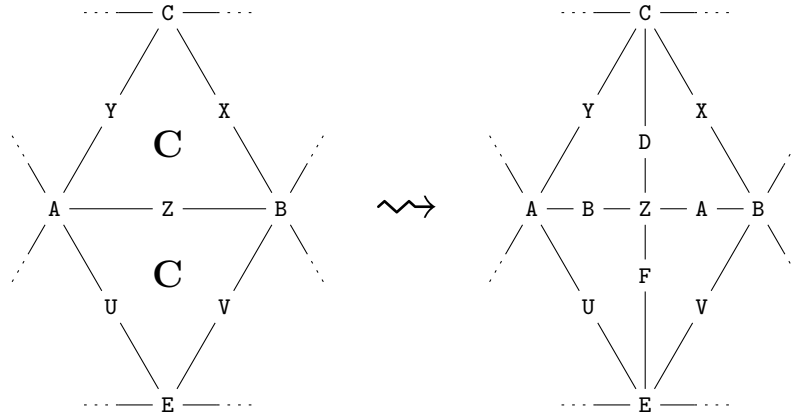


Fig. 6. Splitting 2 adjacent Ceva-triangles.

translating every Ceva-Menelaus-proof into a pure Menelaus-proof, it at atleast shows that pure Menelaus-proofs must be stronger than pure Ceva-proofs.

4.3 Summary of the Results

In total we get the following relations between the proving methods final polynomials (**P**), binomial proofs (**B**), Ceva-Menelaus-proofs (**CM**), quad-proofs (**Q**), pure Menelaus-proofs (**M**) and pure Ceva-proofs (**C**), where “ \Rightarrow ” means “at least as powerful as”.

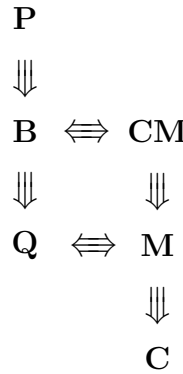


Fig. 7. Hierarchy of proving techniques.

5 Two illustrative examples

We now will exemplify the translation between the proving methods by two simple, but suitably examples: Desargues' and Pappus' Theorems. We purposely chose the most elementary theorems, since there the connections between the approaches can be seen in a most transparent way.

5.1 Desargues' Theorem

Desargues' Theorem can be — and has been — shown using all presented techniques. In particular, it can be proven using:

1. A tiling of the sphere consisting of 6 quadrangles (a cube) as shown in [7],
2. A tiling of the sphere consisting of 4 Menelaus-triangles (a tetrahedron) as shown in [8] or
3. 10 binomial equations coming from 10 collinear point triples and Grassmann-Plücker-relations also shown in [8, 9].

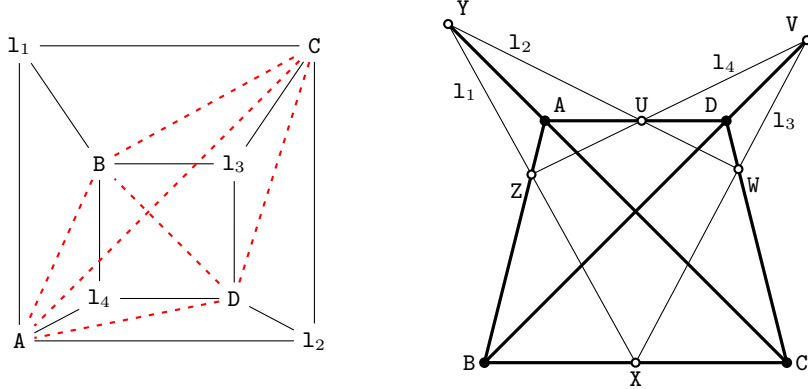


Fig. 8. Tiling proofs for Desargues' theorem.

We start with a the quad-proof whose combinatorics corresponds to the cube (Figure 8, left). The eight vertices of the cube have to be considered as the vertices of a bipartite graph. Half of them (A, \dots, D) representing points and the other half (l_1, \dots, l_4) representing lines. The consistency condition for each of the six faces corresponds to one incidence. For instance the face with vertices B, C, l_1, l_3 corresponds to the point X in the Figure 8 (right) at which the lines l_1, l_3, \bar{BC} meet. In that sense every face of the cube gets associated with a point in Desargues' Theorem and $A \dots B, U \dots Z$ form the ten points of the theorem.

We now translate the coherent face conditions into a collection of binomial determinant expressions. For that we must express the lines as spans of two points. In our example for each line we take any two of the three points incident

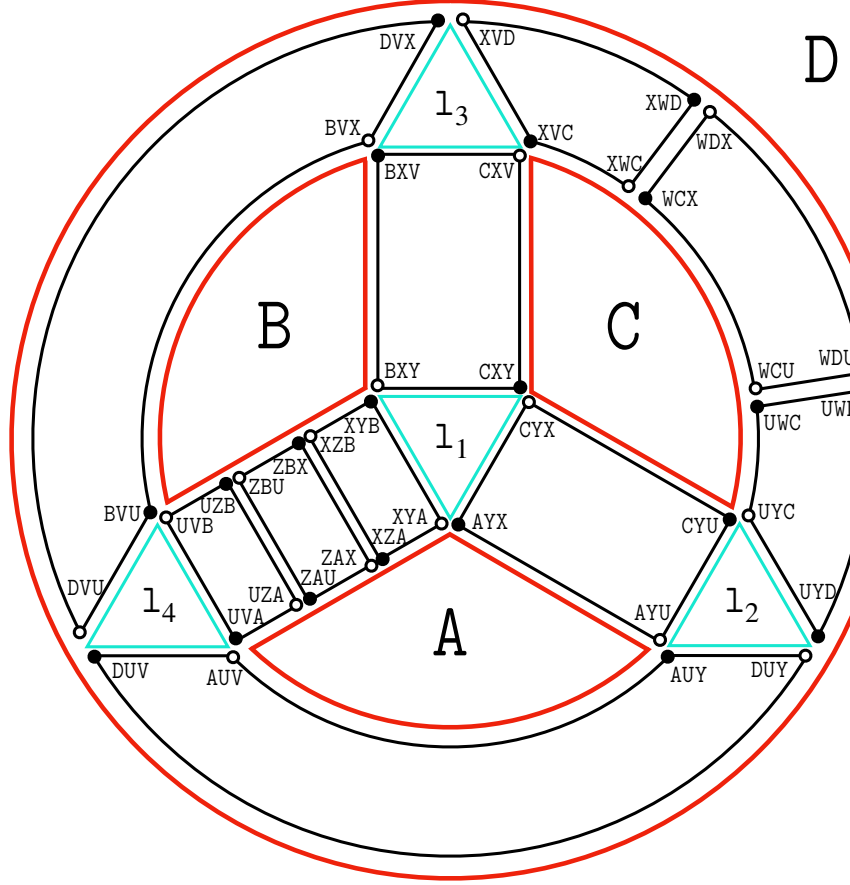


Fig. 9. The big picture.

to it. While the approach from Section 3.1 would actually generate 18 binomial equations from the quad-proof, the specific combinatorial structure allows us to “take a shortcut” and translate four of the quadrangles using only *one* binomial equation each, by describing the lines directly as joins of the incidence points of adjacent quadrangles. We get

$$\begin{aligned}
 \text{coherent quadrangle } A, l_2, C, l_1 &\iff [A, Y, X][C, Y, U] = [A, Y, U][C, Y, X] \\
 \text{coherent quadrangle } C, l_3, B, l_1 &\iff [C, X, Y][B, X, V] = [C, X, V][B, X, Y] \\
 \text{coherent quadrangle } B, l_3, D, l_4 &\iff [B, V, U][D, V, X] = [B, V, X][D, V, U] \\
 \text{coherent quadrangle } D, l_2, A, l_4 &\iff [D, U, V][A, U, Y] = [D, U, Y][A, U, V]
 \end{aligned}$$

for four of the faces. We collect the remaining brackets by translating the equations coming from the two quadrangles using the method from 3.1.

$$\begin{aligned}
 \text{coherent quadrangle } A, l_1, B, l_4 &\iff [A, U, V][B, X, Y] = [A, X, Y][B, U, V] \\
 &\iff [U, V, A][U, Z, B] = [U, V, B][U, Z, A] \text{ and} \\
 &\quad [X, Y, B][X, Z, A] = [X, Y, A][X, Z, B] \text{ and} \\
 &\quad [Z, A, U][Z, B, X] = [Z, A, X][Z, B, U] \\
 \text{coherent quadrangle } C, l_2, D, l_3 &\iff [C, X, V][D, U, Y] = [C, U, Y][D, X, V] \\
 &\iff [X, V, C][X, W, D] = [X, V, D][X, W, C] \text{ and} \\
 &\quad [U, Y, D][U, W, C] = [U, Y, C][U, W, D] \text{ and} \\
 &\quad [W, C, X][W, D, U] = [W, C, U][W, D, X]
 \end{aligned}$$

This results in 10 binomial equations cancelling each other out. In this collection of 10 binomial equations each equation encodes exactly one collinearity of the underlying Desargues' Theorem. Thus we have a binomial proof. The cancellation pattern in the quad-proof directly translates to the proving structure in the binomial proof.

Figure 9 shows the situation in a more wholistic way. There ten quadrilateral regions are shown (black). Each vertex corresponds to the occurrence of one bracket in one binomial equation. Black vertices correspond to brackets occurring on the left. White vertices occur on the right of the equations. The vertices are labelled with the letters of the corresponding bracket. The cancellation property corresponds to the fact that whenever a black and a white vertex meet they are labelled by the same letters.

Each black edge can be considered as a ratio of the form $[OPQ]/[OPR]$ (dividing its black end by its white end). Thus each edge represents a length ratio. There are four red regions in the image labelled A, \dots, D . They represent the *points* in the original quad-proof. Note that each vertex adjacent to such a region contains the corresponding letter. The blue triangles represent the *lines* in the quad-proof. The vertices adjacent to such a triangle all share two points. These two points span the corresponding line.

Finally, we can read off the corresponding Ceva-Menelaus proof. For this we only have to focus on the green triangles. They will be considered as the triangles in a Menelaus proof. Each pair of triangles is glued along two edges that are connected by a long black region (either consisting of one or of three quadrilateral cells). The two segments at the end of such a region represent the same length ratio. For instance the region connecting l_1 and l_4 connects to l_1 by $[XYB]/[XYA]$ and connects to l_4 by $[UVA]/[UVB]$. Both fractions represent the same length ratio $\overrightarrow{ZA}/\overrightarrow{ZB}$ (one of them as a reciprocal of the other). This is the ratio in which the lines l_1 and l_4 cut the line \overline{AB} .

If we collect the products of the ratios for the 4 Menelaus triangles ABC with line l_1 , ACD with line l_2 , BCD with line l_3 and ABD with line l_4 , then their

Menelaus-equations are equivalent to the obvious identities

$$\begin{aligned}
 \text{ABC with } l_1 \iff & \frac{[X, Y, A]}{[X, Y, B]} \cdot \frac{[X, Y, B]}{[X, Y, C]} \cdot \frac{[X, Y, C]}{[X, Y, A]} = 1 \iff \frac{\overrightarrow{AZ}}{\overrightarrow{ZB}} \cdot \frac{\overrightarrow{BX}}{\overrightarrow{XC}} \cdot \frac{\overrightarrow{CY}}{\overrightarrow{YA}} = -1, \\
 \text{ACD with } l_2 \iff & \frac{[U, Y, A]}{[U, Y, C]} \cdot \frac{[U, Y, C]}{[U, Y, D]} \cdot \frac{[U, Y, D]}{[U, Y, A]} = 1 \iff \frac{\overrightarrow{AY}}{\overrightarrow{YC}} \cdot \frac{\overrightarrow{CW}}{\overrightarrow{WD}} \cdot \frac{\overrightarrow{DU}}{\overrightarrow{UA}} = -1, \\
 \text{BCD with } l_3 \iff & \frac{[X, W, C]}{[X, W, B]} \cdot \frac{[X, W, B]}{[X, W, D]} \cdot \frac{[X, W, D]}{[X, W, C]} = 1 \iff \frac{\overrightarrow{CX}}{\overrightarrow{XB}} \cdot \frac{\overrightarrow{BV}}{\overrightarrow{VD}} \cdot \frac{\overrightarrow{DW}}{\overrightarrow{WC}} = -1, \\
 \text{ABD with } l_4 \iff & \frac{[U, V, B]}{[U, V, A]} \cdot \frac{[U, V, A]}{[U, V, D]} \cdot \frac{[U, V, D]}{[U, V, B]} = 1 \iff \frac{\overrightarrow{BZ}}{\overrightarrow{ZA}} \cdot \frac{\overrightarrow{AU}}{\overrightarrow{UD}} \cdot \frac{\overrightarrow{DV}}{\overrightarrow{VB}} = -1.
 \end{aligned}$$

Now these fractions contain *exactly* the same brackets in the numerator and denominator as the equations coming from the quadrangles on each side of the equality. Thus we have a Menelaus proof. Hence Figure 9 visualizes the structure of all three proofs in one single picture.

5.2 Pappus' Theorem

In the last section we have seen, that binomial equations seem to be the “building blocks” for quad-proofs, in the sense that each quadrangle can be expressed by at most 3 binomial equation. On the other hand we have seen, that binomial proofs and Ceva-Menelaus proofs are in a certain sense “dual” to each other, as one lives in the gaps of the other. We continue with one of the most fundamental projective incidence theorems: Pappus' Theorem.

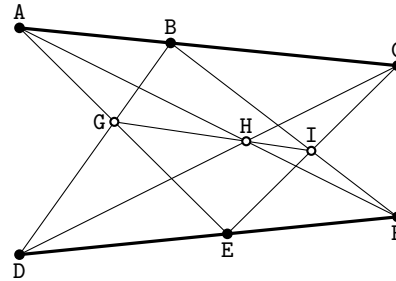


Fig. 10. The theorem of Pappus.

Again, both [7] and [8] give tiling-proofs for it and we analyze how they relate to each other and reveal some additional structure, which was “hidden” in the proofs of Desargues' theorem. A similar analysis but without the quad-proofs

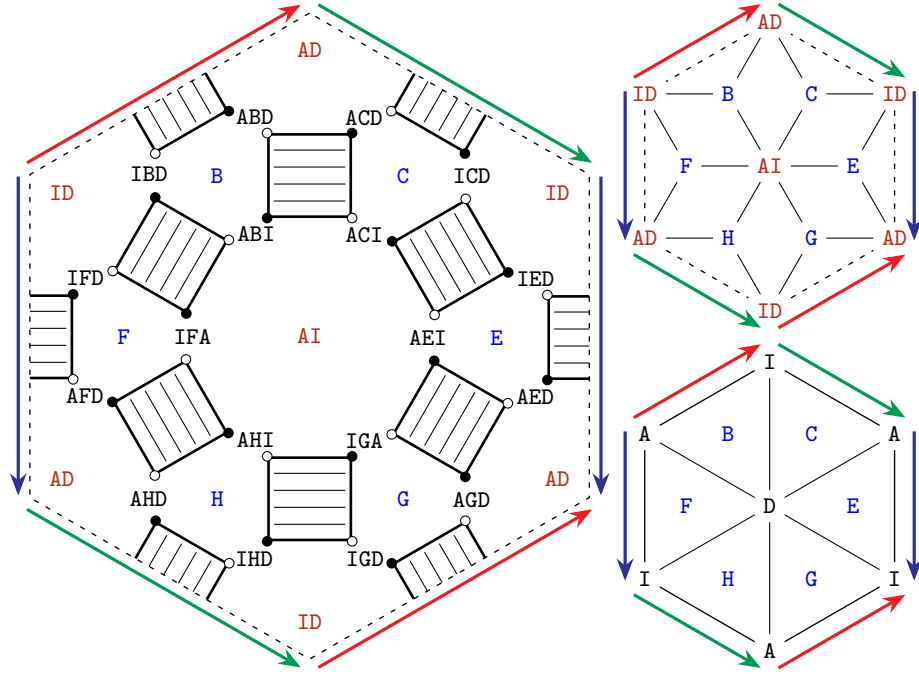


Fig. 11. The proofs of Pappos's theorem visualized.

was already performed in [1]. We will start from the binomial proof:

$$\begin{aligned}
 ABC \text{ collinear} &\iff [A, B, D][A, C, I] = [A, B, I][A, C, D] \\
 AHF \text{ collinear} &\iff [A, H, D][A, F, I] = [A, H, I][A, F, D] \\
 AEG \text{ collinear} &\iff [A, E, D][A, G, I] = [A, E, I][A, G, D] \\
 DCH \text{ collinear} &\iff [D, C, A][D, H, I] = [D, C, I][D, H, A] \\
 DFE \text{ collinear} &\iff [D, F, A][D, E, I] = [D, F, I][D, E, A] \\
 DGB \text{ collinear} &\iff [D, G, A][D, B, I] = [D, G, I][D, B, A] \\
 IGH \text{ collinear} &\iff [I, G, D][I, H, A] = [I, G, A][I, H, D] \\
 IBF \text{ collinear} &\iff [I, B, A][I, F, D] = [I, B, D][I, F, A] \\
 ICE \text{ collinear} &\iff [I, C, D][I, E, A] = [I, C, A][I, E, D]
 \end{aligned}$$

As before, any of the 9 equations is implied by the other 8. Now, in the same way as in Figure 9 we will depict the binomial equations as small rectangles, glued together wherever they share a bracket. While the proofs for Desargues' theorem lived on a sphere the resulting structure here lives on a torus which can easily be seen on the left in Figure 5.2. As we already saw in the last example, the holes correspond to points or lines, depending on how many points in the brackets are shared. For example, the top left triangle has the brackets ABD, ABI

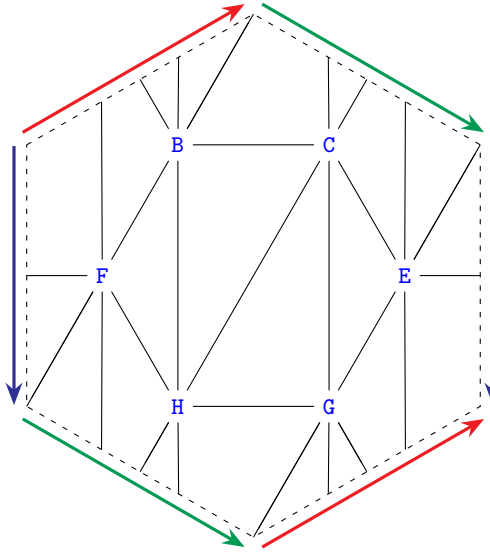


Fig. 12. Proof of Pappos's theorem using 12 Menelaus triangles.

and BDI as vertices, so all of them contain the point B . On the other hand, all 6 vertices of the hexagon in the middle share the points A and I , so this gives us the line spanned by them. This way we can immediately read of quadrilateral-tiling proof: We just need to create quadrangles with points and lines as vertices, as seen in Figure 5.2 top right. Extracting a Ceva-Menelaus-Proof from this picture is just as easy, as the triangles whose share 1 point correspond exactly to Ceva-triangles with the shared point as “Ceva-point”. In particular, e.g. the top left triangle $ABD \rightarrow IBD \rightarrow ABI$ corresponds to the Ceva-triangle $I \rightarrow A \rightarrow D$ with the point B in the middle, yielding:

$$1 = \frac{[A, B, D]}{[I, B, D]} \frac{[I, B, D]}{[A, B, I]} \frac{[A, B, I]}{[A, B, D]},$$

which is equal to the length ratios along the edges of the triangle. Doing this for all 6 triangles we end up with the pure Ceva-proof in the bottom right of Figure 5.2. In fact, these two proofs were already presented in [7] and [8], respectively and are now shown to be “the same proof” in the sense of coming from the same binomial cancellation pattern.

If we compare Figures 9 and 5.2 again, we can see that in the first one we saw triangular holes where all brackets at the vertices shared 2 points and in the second one we saw triangular holes where all brackets at the vertices vertices shared only 1 point. We then saw that these holes can be interpreted as Menelaus-respectively Ceva-triangles. We now focus on the non-triangular holes. They will lead to a pure Menelaus-proof whose existence has been claimed in Section 4. If we take a close look at the 3 hexagonal holes in 5.2 we can see, that all brackets

at their vertices share the same 2 points: A and I , for the central one, A and D for the one in the top and I and D for the one in the bottom. So actually, each of those can be triangulated using 4 Menelaus-triangles resulting in another proof of Pappus's theorem using 12 Menelaus triangles, which happens to be exactly one of Menelaus proofs we would get applying the translation procedure from Section 4.

This method in fact works for all binomial proofs! The proof in [1] showing that Ceva-Menelaus-proofs and binomial proofs are equivalent, forms chains of binomial equations (the black rectangles in Figure 5.2) and uses cycles of unmatched edges to fit Ceva- and Menelaus-triangles inside. In fact there are always 2 possibilities to do this, yielding at least 2 Ceva-Menelaus-proofs per binomial proof.

6 Three three-dimensional examples

One might wonder, how the different concepts generalize to higher dimensions. In [7] Fomin and Pylyavskyy give several examples of quad-proofs that can be considered as proofs for 3-dimensional incidence theorems. Also in [9] biquadratic final polynomial proofs are given for some 3D incidence theorems. We here exemplify how the Ceva/Menelaus Method can be interpreted in a 3-dimensional context. For that, we first have to explore how the theorems of Ceva and Menelaus can be transformed to higher dimensions. We restrict ourselves to the 3-dimensional case.

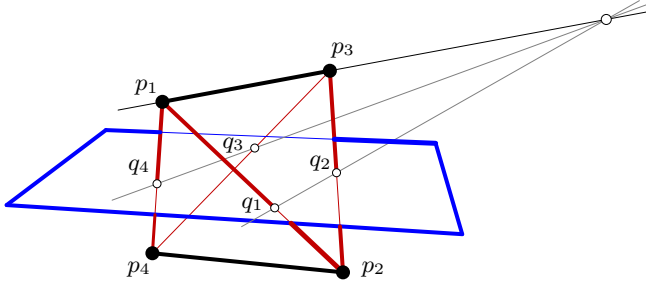


Fig. 13. 3D-Menelaus

There are several ways to generalize Ceva's and Menelaus's theorem to higher dimensions. Here we will refer to the following two versions, whose proofs are immediate.

Theorem 1. (3D Menelaus): *Let p_1, \dots, p_4 be four non coplanar points in three-space. Consider a plane in general position H and the intersections $q_i := H \cap$*

$\overline{p_i, p_{i+1}}$ (indices mod 4). Then we have (with oriented distances):

$$\frac{|p_1, q_1|}{|q_1, p_2|} \cdot \frac{|p_2, q_2|}{|q_2, p_3|} \cdot \frac{|p_3, q_3|}{|q_3, p_4|} \cdot \frac{|p_4, q_4|}{|q_4, p_1|} = 1$$

Similarly we have a version of Ceva's Theorem.

Theorem 2. (3D Ceva): Let p_1, \dots, p_4 be four non coplanar points in three space. Consider one further point a . For the line $\overline{p_i, p_{i+1}}$ consider the plane $H_i := a \vee p_{i+2} \vee p_{i+3}$ and the intersection point $q_i := H_i \cap \overline{p_i, p_{i+1}}$ (indices mod 4). Then we have:

$$\frac{|p_1, q_1|}{|q_1, p_2|} \cdot \frac{|p_2, q_2|}{|q_2, p_3|} \cdot \frac{|p_3, q_3|}{|q_3, p_4|} \cdot \frac{|p_4, q_4|}{|q_4, p_1|} = 1$$

The proofs of these two theorems follow exactly the same reasoning as in the 2D case presented in [8]. The situation of the 3D-Menelaus is shown in Figure 13. The blue plane plays the role of the plane H , cutting the edges of a 4-cycle in the tetrahedron. The image also indicates a simple argument for the multiratio equation. First observe that the three lines $q_1 \vee q_2$, $q_3 \vee q_4$ and p_1, p_3 must meet in a point since they are the mutual intersections of three planes H , $p_1p_2p_3$, $p_1p_4p_3$. Now consider the drawing literally as an orthogonal projection of the 3D situation. Then the 4-cycle can be considered as a version of two 2D Menelaus configurations glued along the edge p_1p_3 along which the joint factor cancels. From there it is also immediate to arrive at the corresponding 3D-Ceva theorem. For this observe that both Ceva and Menelaus have the same multiration (= 1) hence the four points that split the cycle can as well be interpreted as Menelaus points or Ceva points. In other words if q_1, \dots, q_4 satisfy the Menelaus condition (they are coplanar) they also satisfy the Ceva condition (the planes $p_1p_2q_3$, $p_2p_3q_4$, $p_3p_4q_1$, $p_4p_1q_2$ meet in a point). The intersection $p_1p_2q_3 \wedge p_3p_4q_1$ is the line q_3q_1 and the intersection $p_3p_4q_1 \wedge p_4p_1q_2$ is the line q_2q_4 . Since the four points q_i are coplanar these two lines (and hence the four planes) must intersect. The argument can easily be reversed.

We will call these two configurations Menelaus and Ceva configurations, respectively. These CM 4-gons will be used in our manifold proofs. Figure 14 shows the labelings of these 4-gons if we use them in a base graph. The left picture shows a Menelaus quadrilateral. Where we assume that the vertices of the tetrahedron are A, \dots, D and the plane H is spanned by three points XYZ . The right picture shows the Ceva situation with a tetrahedron A, \dots, D and an interior point E .

6.1 The Sixteen Point Theorem

We now consider a spatial theorem that is known under the name *Sixteen Point Theorem*. Already in a very early preprint [3] on bi-quadratic final polynomials the following two incidence theorems, their bi-quadratic final polynomials, and



Fig. 14. The labelings of 3D Ceva and Menelaus quadrangles.

their regular combinatorial properties was mentioned. We *revisit* these structures here in order to emphasize how they can be translated into manifold proofs.

The 16 Point Theorem actually can be interpreted as a theorem about two collections of 4-lines and their 16 points of potential mutual intersections. Consider Figure 15 for the geometric configuration.

Theorem 3. *Let $l_1, \dots, l_4, m_1, \dots, m_4$, be two sets of lines (such that all 8 lines are distinct). If 15 of the 16 pairs of lines $\{l_i, m_j\}$ are incident then also the final one is incident.*

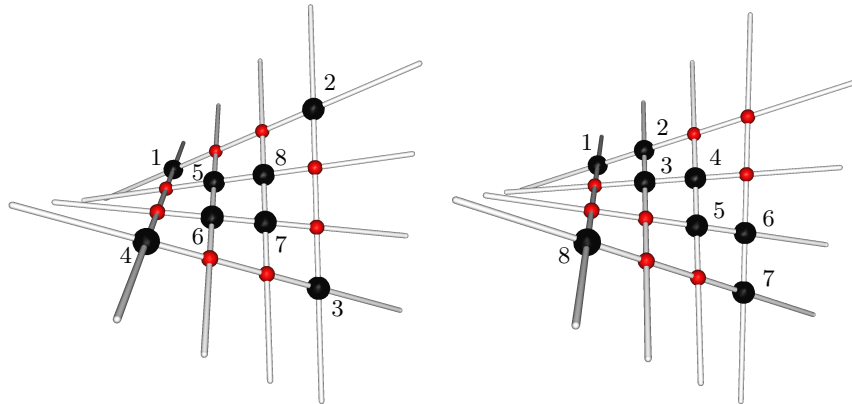


Fig. 15. Two versions of the 16-points theorem.

One can rephrase the theorem as an incidence theorem on 8 points and 8 coplanarity relations. This can be done in two combinatorially non-isomorphic ways. They are depicted in the two images of Figure 15. The points of the configuration are shown as black dots. Each line is spanned by exactly two such points. Thus each black point already encodes an incidence of two lines. The small red dots correspond to the 8 remaining incidences. The two lines $I \vee J$ and $K \vee L$ are incident if and only if I, J, K, L are coplanar. Hence in each of the two versions seven coplanarities imply an eighth one. The combinatorics of both types amazingly can also be interpreted as a torus consisting of 8 quadrilaterals.

Figure 16 shows the combinatorics for the two cases. Each square represents a coplanarity between points.

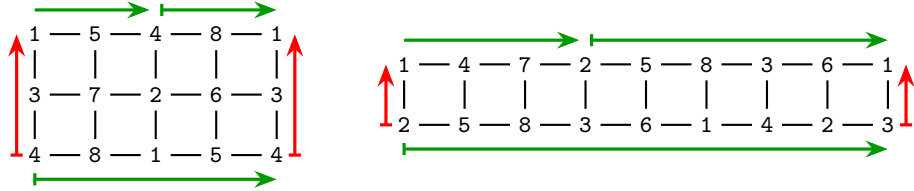


Fig. 16. The combinatorics of the two versions of the 16 point theorem.

In [9] bi-quadratic final polynomials for both cases were given. We now translate these bi-quadratic final polynomials into CM-proofs and into quad-proofs. We start with the case associated to the structure in the left of Figures 15 and 16. A final polynomial for this one is given by (see [9]):

$$\begin{aligned}
 [1253][1264] &= [1254][1263] & \Leftarrow h(1526) \\
 [2361][2374] &= [2364][2371] & \Leftarrow h(2637) \\
 [3451][3462] &= [3452][3461] & \Leftarrow h(6453) \\
 [1463][1472] &= [1462][1473] & \Leftarrow h(6471) \\
 [3471][3482] &= [3472][3481] & \Leftarrow h(4837) \\
 [1452][1483] &= [1453][1482] & \Leftarrow h(4815) \\
 [1273][1284] &= [1274][1283] & \Leftarrow h(8271) \\
 [2354][2381] &= [2351][2384] & \Rightarrow h(8253)
 \end{aligned}$$

Inspecting the structure and arranging the bi-quadratic equations along a manifold like structure yields the picture in Figure 17 (left). The image has to be interpreted as a torus, with opposite edges identified. Each shaded cell corresponds to a bi-quadratic equation with black vertices appearing on the left and white vertices appearing on the right of the equation. Obviously at each bracket a white and a black vertex meet yielding the decisive cancellation pattern. The regularity of this cancellation pattern was already mentioned in [3].

Surrounded by the squares of the bi-quadratic equations there are eight other *empty* squares in this diagram. The labels in their center correspond to the points that are shared by the four adjacent brackets. There are cells labelled by one point that correspond to a 3D Ceva cycle and cells labelled by three points corresponding to a 3D Menelaus cycle. It can be easily checked, that these cycles indeed correspond to Ceva and Menelaus configurations in the original incidence configuration. In the Menelaus-like cells the three points span the cutting plane for the Menelaus configuration. In the Ceva cell the one letter in the inside characterizes the one additional point needed for a Ceva configuration.

As before, we may consider the binomial equations as glue between two Ceva or Menelaus cells. Each such bi-quadratic square can be used to encode the identity of two opposite edges and we can decide which pair of edges is identified.

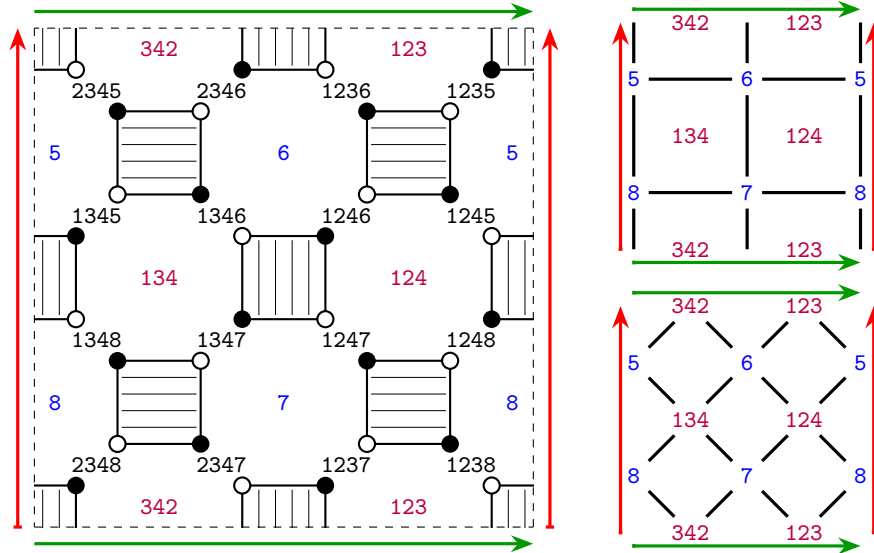


Fig. 17. Structure diagrams for the manifold proofs of the theorem.

In the drawing of Figure 17 (left) the squares are shaded indicating a direction. We assume that the squares are used to identify the ratios along the edges in the same direction as the shading. For instance the upper left square whose vertices are 2345, 2346, 1346, 1345 is used to encode the ratio equivalence $\frac{[2345]}{[2346]} = \frac{[1345]}{[1346]}$. Doing all these identifications turns the diagram into a CM-proof that entirely consists of Menelaus configurations. It is shown in Figure 17 (right, top). This CM-proof simply consists of a 2×2 grid with identified opposite edges. It has the topology of a torus. Each cell corresponds to a 3D Menelaus configuration. If we consequently identify the other edges of the bi-quadratic squares. We get a similar proof where each cell is a 3D Ceva configuration. Each such situation is already completely determined by the diagrams in Figure 18. and the dimension in which the configuration should take place.

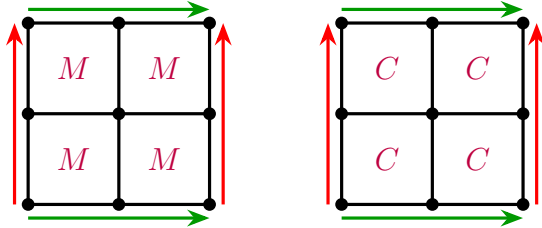


Fig. 18. Two proving schemes for the CM-proof.

We next show how the structure can be used to create a quad-proof. The corresponding structure is shown in Figure 17 (right, bottom). Again the underlying manifold is a torus. This time consisting of eight 4-gons. The vertices the manifold consist of are 4 points and 4 hyperplanes. The hyperplanes correspond to the red labels with 3 letters. The vertices are the blue labels with one letter. The same manifold scheme was also given in [7] (Theorem 5.5).

Next we give the corresponding proving schemes for the incidence theorem shown in Figure 16 on the right, the second way to express the 16 point theorem. Also here in [3] a bi-quadratic final polynomial was given. Instead of listing the equations, we immediately start with the graphical representation for the bi-quadratic proof. It is shown in Figure 19. To make it easier to see the structure we show a region that corresponds to *two* full covers of the underlying torus. The rectangular dashed region corresponds to one full cover of the torus. To obtain the torus in that region the left and right side have to be identified and to bottom and top side are identified with a shift of 2 units. Again the shaded squares represent binomial equations and the black and white points meeting at the corners represent the same bracket (once on the left and once on the right of the bi-quadratic equations).

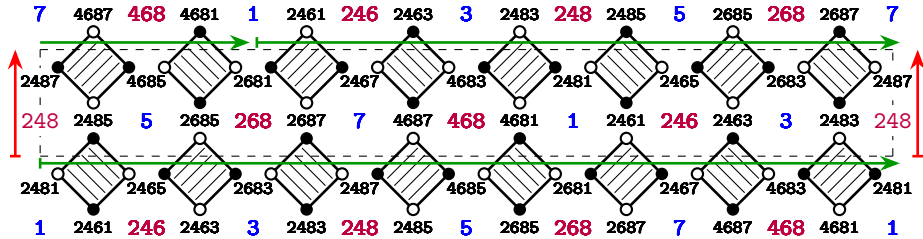


Fig. 19. Proof for the second version of the 16 point theorem.

In a completely analogous way to the previous example we can extract CM-proofs and quad-proofs from this scheme. The corresponding schemes for the quad-proof and Menelaus proof is shown in Figure 20.

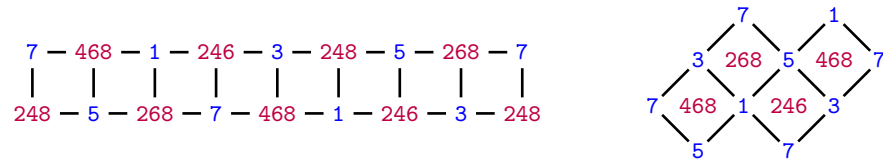


Fig. 20. A quad-proof and Menelaus proof for the second version of the 16 point theorem.

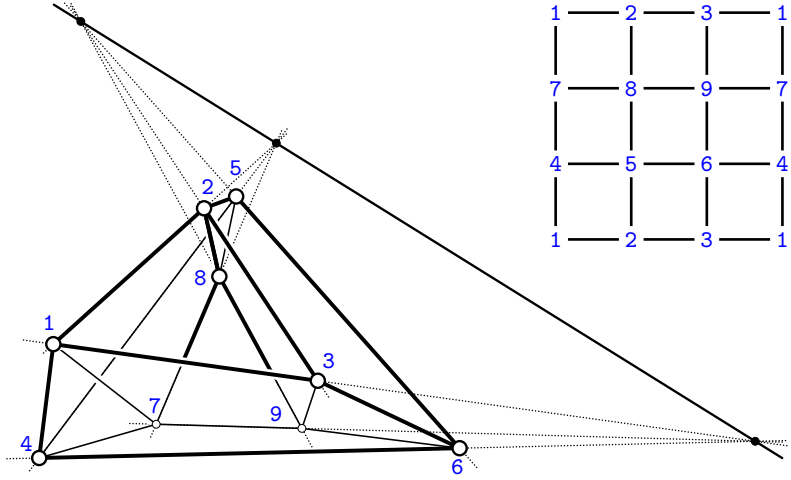


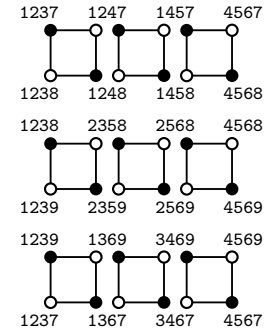
Fig. 21. Geometry and combinatorics of the Toblerone Theorem.

6.2 The 3×3 torus

Our final example is sometimes jokingly called the Toblerone Torus, since it can be assembled from three Toblerone boxes out of which one builds a triangular frame. It is the torus formed by a grid of 3×3 quadrilaterals. It has 9 vertices. If eight of the quadrilaterals are flat the final one is flat automatically. Figure 21 shows a projectively correct 2D drawing of this configuration along with its combinatorial structure.

Again in [9] a bi-quadratic final polynomial for this incidence theorem was provided. We present this final polynomial here in an pre-structured form. We separate it into three blocks. Within each block the red and the green parts cancel directly and we have a chain of three bi-quadratic equations of which only the outer parts –the black brackets in the equations– are relevant (similar to the chains we observed in Figure 9). We show these blocks along with a graphical representation of the cancellation chains that belong to each block.

$$\begin{aligned}
 [1273][1284] &= [1274][1283] \quad \Leftarrow \quad h(7812) \\
 [1458][1427] &= [1428][1457] \quad \Leftarrow \quad h(1245) \\
 [4571][4586] &= [4576][4581] \quad \Leftarrow \quad h(4578) \\
 [2381][2395] &= [2385][2391] \quad \Leftarrow \quad h(8923) \\
 [2569][2538] &= [2539][2568] \quad \Leftarrow \quad h(2356) \\
 [5682][5694] &= [5684][5692] \quad \Leftarrow \quad h(5689) \\
 [3192][3176] &= [3196][3172] \quad \Leftarrow \quad h(9741) \\
 [3647][3619] &= [3617][3649] \quad \Leftarrow \quad h(3164) \\
 [6493][6475] &= [6495][6473] \quad \Rightarrow \quad h(6497)
 \end{aligned}$$



Since only the terminal edges of these chains can form ratios that are needed for either CM-proofs or quad-proofs we can immediately collapse these chains and focus on the resulting equations. Doing so we are left with the following three equations (digits have been sorted while taking care of the signs of the determinants).

$$\begin{aligned} [1237][4568] &= [1238][4567] \\ [1238][4569] &= [1239][4568] \\ [1239][4567] &= [1237][4569] \end{aligned} \quad (5)$$

The amazingly difficult part of translating these equations into a CM-proof or a quad-proof comes from the fact that there is hardly any structure left that relates these equations to the geometry of the theorem. Let us first interpret the structure as a quad-proof.

We first consider the equation

$$[1237][4568] = [1238][4567] \quad (6)$$

and its geometric relevance. It encodes a geometric relation between the planes spanned by 123, 456 and the line spanned by 78. It is exactly the type of equation given by the equation (3), the basic building block of a quad-proof. It holds if the join of 7 and 8 hits the intersection line of the planes 123 and 456. The situation is depicted in Figure 22 on the left. Thus our three equations can be directly interpreted as a quad-proof, representing a very simple configuration. The underlying manifold consists of 3 quadrangles that form a spherical structure as indicated in Figure 23 (left). In that picture also the exterior face has to be considered as a quadrangle.

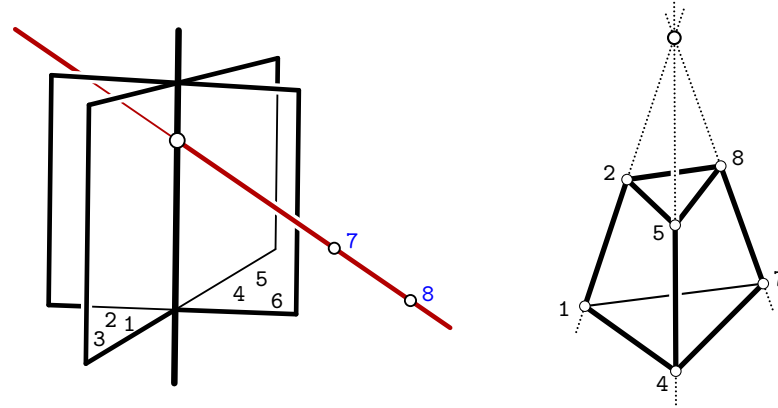


Fig. 22. Geometric relations to interpret equation (6).

Why does this manifold structure proof our theorem? For this again consider the equation $[1237][4568] = [1238][4567]$. and consider the three coplanari-

ties 1245, 1278 and 4578. They are part of our geometric configuration of the Toblerone torus. Since any three planes meet in a point (perhaps infinite) this implies that the lines $\overline{12}$, $\overline{45}$, $\overline{78}$ meet in a point. This in turn is exactly encoded by equation (6), where 3 and 6 play the role of auxiliary points in suitably general position. Conversely, if (6) holds and we know that 1245, 1278 are coplanar we can conclude that 4578 is coplanar as well. These two statements immediately translate into the fact that the quad-manifold associated to (5) proves the Toblerone torus theorem: If eight coplanarities are satisfied then two of the equations hold. This implies that the third equation holds this together with the two remaining coplanarities implies the conclusion of the theorem.

Finally, it remains to interpret the equations in terms of a CM-proof. For this we again can consider the equations in (5) as glue between triangle edges. The manifold is as trivial as it could be. It just consists of two copies of the triangle 789 as Menelaus triangles and glued along their edges. One instance is assumed to be cut by the plane 123. The other instance is assumed to be cut by 456. The interplay of the geometric situation and the CM-proof can be understood by reconsidering Figure 21. The three triangles 123, 456 and 789 are boundary a cycle of the torus. Cutting 789 with a plane 123 produces additional points on the lines that support the edges (one can see them in Figure 21). They are the three points of the perspective line indicated in this figure. The almost trivial CM-proof manifold states that if one chooses plane 789 such that it passes through the intersection line of 123 and 456 then the following holds. If we have $78 \wedge 123 = 78 \wedge 456$ and $89 \wedge 123 = 89 \wedge 456$ then we automatically have $79 \wedge 123 = 79 \wedge 456$. This is exactly what we need for the incidence theorem to hold.

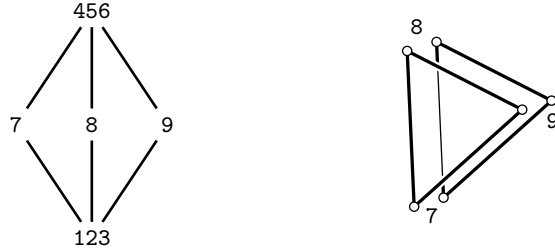


Fig. 23. Quad proof and CM-proof for the Toblerone torus.

It is remarkable that CM-proofs that produce a void statement in a 2D interpretation produce an interesting incidence theorem when interpreted in a 3D framework. We do not claim that thinking of the proofs in that case in terms of quad-proofs or CM-proofs is conceptually simpler than using a bi-quadratic framework. However, it is nice to see that even these highly degenerate proving manifolds smoothly fit in our general interplay of the three different proving techniques.

References

1. Apel, S., Richter-Gebert, J.: Cancellation Patterns in Automatic Geometric Theorem Proving. In: Automated Deduction in Geometry (2010)
2. Bokowski, J., Richter(-Gebert), J.: On the finding of final polynomials, *Eur. J. Comb.*, 11 (1990), 21–34.
3. Bokowski, J., Richter(-Gebert), J.: On the classification of non-realizable oriented matroids – Part II Properties, Preprint 1345, TU Darmstadt, (1990), 16 pages.
4. Bokowski, J., Sturmfels, B.: Computational Synthetic Geometry. Lecture Notes in Mathematics **1355** Springer, Heidelberg (1989)
5. Pylavskyy, P., Skopenkov, M.: Incidences, tilings, and fields. 2025. arXiv: 2505.02229v1
6. Kutzler, B., Stifter, S., 1986. On the application of Buchberger's algorithm to automated geometry theorem proving. *J. Symbolic Comput.* 2,1986, 389–398.
7. Fomin, S., Pylavskyy, P.: Incidences and Tilings. 2023. arXiv: 2305.07728
8. Richter-Gebert, J.: Meditations on Ceva's Theorem. In: The Coxeter Legacy (2006), pp. 227–254
9. Richter-Gebert, J.: Mechanical theorem proving in projective geometry. *Ann Math Artif Intell* 13, 139–172 (1995). <https://doi.org/10.1007/BF01531327>
10. Wu, W.T.: Basic Principles of Mechanical Theorem Proving in Geometries, Vol. I: Part of Elementary Geometries. Springer (Original work published 1984. Science Press, Beijing), 1994.